

Article

Colloids in Thermokarst Lakes along a Permafrost and Climate Gradient of Permafrost Peatlands in Western Siberia Using In Situ Dialysis Procedure

Rinat M. Manasyrov ^{1,*}, Artem G. Lim ¹, Ivan V. Krickov ¹, Tatiana V. Raudina ¹, Danil G. Kurashev ¹,
Liudmila S. Shirokova ^{2,3} and Oleg S. Pokrovsky ³

¹ BIO-GEO-CLIM Laboratory, Tomsk State University, 36 Lenina av., Tomsk 634050, Russia; lim_artiom@mail.ru (A.G.L.); krickov_ivan@mail.ru (I.V.K.); tanya_raud@mail.ru (T.V.R.); danil_kurashev@mail.ru (D.G.K.)

² Federal Center for Integrated Arctic Research, Institute of Ecological Problem of the North, 23 Nab. Severnoi Dviny, Arkhangelsk 163000, Russia; lshirokova@ya.ru

³ Geosciences and Environment Toulouse, UMR 5563 CNRS, 14, Avenue Edouard Belin, 31400 Toulouse, France; oleg.pokrovski@get.omp.eu

* Correspondence: rmanasyrov@gmail.com

Abstract: Thermokarst lakes in the Western Siberian Lowland (WSL) are major environmental factors controlling organic carbon and trace metal storage in inland waters and greenhouse gas emissions to the atmosphere. In contrast to previously published research devoted to lake hydrochemistry, hydrobiology, sedimentary carbon, and processes controlling the lake total dissolved (<0.45 μm) solute composition, the colloidal forms of organic carbon (OC), and related elements remain poorly known, especially across the permafrost gradient in this environmentally important region. Here we sampled 38 thermokarst lakes in the WSL, from the continuous to the permafrost-free zone, and we assessed both the total (<0.45 μm) and low-molecular-weight (<1 kDa) concentrations of 50 major and trace elements using conventional filtration and in situ dialysis. We aimed at quantifying the relationships between the colloidal content of an element and the lake surface area, permafrost coverage (absent, sporadic, isolated, discontinuous, and continuous), pH, and the concentrations of the main colloidal constituents, such as OC, Fe, and Al. There was a positive correlation between the lake area and the contents of the colloidal fractions of DOC, Ni, rare earth elements (REE), and Hf, which could be due to the enhanced mobilization of OC, trace metals, and lithogenic elements from silicate minerals in the soil porewater within the lake watershed and peat abrasion at the lake border. In all permafrost zones, the colloidal fractions of alkalis and alkaline-earth metals decreased with an increase in lake size, probably due to a decrease in the DOC concentration in large lakes. There was an increase in the colloidal fractions of DOC, Fe, Al, trivalent and tetravalent trace cations, Mn, Co, Ni, As, V, and U from the southern, permafrost-free zone to the northern, permafrost-bearing zones. This observation could be explained by an enhanced feeding of thermokarst lakes by suprapermafrost flow and the thawing of dispersed peat ice in the northern regions. Considering the large permafrost gradient of thermokarst lakes sampled in the present study, and applying a space-for-time substitution approach, we do not anticipate sizable changes in the colloidal status of DOC or major or trace elements upon climate warming and the permafrost boundary shifting northwards. For incorporating the obtained results into global biogeochemical models of OC, metal micronutrients, and toxicant migration in the permafrost regions, one has to consider the connectivity among lakes, soil waters, and rivers. For this, measurements of lake colloids across the main hydrological seasons, notably the winter period, are necessary.

Keywords: colloids; thermokarst lake waters; Western Siberia; organic carbon; trace element; micronutrients; speciation; size fractionation; bioavailability



Citation: Manasyrov, R.M.; Lim, A.G.; Krickov, I.V.; Raudina, T.V.; Kurashev, D.G.; Shirokova, L.S.; Pokrovsky, O.S. Colloids in Thermokarst Lakes along a Permafrost and Climate Gradient of Permafrost Peatlands in Western Siberia Using In Situ Dialysis Procedure. *Water* **2023**, *15*, 1783. <https://doi.org/10.3390/w15091783>

Academic Editor: Cesar Andrade

Received: 21 March 2023

Revised: 26 April 2023

Accepted: 4 May 2023

Published: 6 May 2023



Copyright: © 2023 by the authors. Licensee MDPI, Basel, Switzerland. This article is an open access article distributed under the terms and conditions of the Creative Commons Attribution (CC BY) license (<https://creativecommons.org/licenses/by/4.0/>).

1. Introduction

The recent attention from the scientific community to high-latitude aquatic systems has essentially been driven by recognizing the overwhelming role of these systems in carbon and greenhouse gas cycles and their high vulnerability to ongoing climate warming and anthropogenic pressure [1–5]. In this regard, of particular interest are continental flatlands (wetlands) that present high storage of both surface and soil water and OC in the form of peat deposits, lake sediments, and dissolved pools. Among these regions, the thermokarst lakes of permafrost peatlands in the Western Siberian Lowland (WSL) are major actors of carbon and metal storage in inland waters [6,7] and greenhouse gas emissions to the atmosphere [8–10]. Due to the high concentration of allochthonous (terrestrial) dissolved organic matter (DOM) originating from peat soils dominating the watersheds of these lakes, the majority of solutes are present in so-called colloidal forms, i.e., having a size between 0.45 μm and 1 nm (or a few kDa). These colloids largely contribute to the total dissolved (<0.45 μm) transport and storage of micronutrients, trace metals, and toxicants, yet the bioavailability and migration capacity of dissolved organic carbon (DOC) and TE cannot be evaluated without assessing the low-molecular-weight (<1 nm or kDa) fraction. In contrast to previously published research devoted to lake hydrochemistry [11–16], hydrobiology [17,18], sedimentary carbon [19,20], and processes controlling total dissolved solute composition in the lake water [21,22], the colloidal status of OC and related elements remain poorly known, especially across the permafrost gradient in this environmentally important region. This contrasts the fairly good knowledge about the colloidal biogeochemistry of OC and related metals acquired in the small surface depressions of thawing permafrost [14,23], WSL rivers [24], soil porewaters [25], dispersed ice [26], and even snowpacks [27]. The interest in characterizing both the conventionally dissolved (<0.22 or 0.45 μm) and low-molecular-weight (<1–3 kDa) fractions of natural waters is double. First, colloids are the main forms of many chemical elements, notably trace micronutrients, pollutants, and geochemical indicators in lake waters. A quantitative understanding of these solutes' migration in lake water and their exchange among the surrounding hydrological systems, soil, sediments, and atmosphere is therefore impossible without assessing the colloidal forms. Second, when studying colloids via size fractionation techniques, one also characterizes the so-called “truly dissolved” and potentially bioavailable species, given that the transport channels of microbial cell walls (10 to 30 Å or 1–3 nm in bacteria, 35 to 50 Å or 3–5 nm in plant cells, [28,29]) are comparable in size to pores of a 1 kDa dialysis membrane, 1–2 nm). Therefore, quantifying the proportion of an element in the colloidal form allows for assessing its bioavailable fraction. This fraction, in turn, controls the trace element toxicity and bioavailability, which is crucially important for establishing the main controlling factors of DOM processing, GHG emissions, and OC storage. However, as stated above, any information on the colloidal and truly dissolved forms of OC and major and trace elements in thermokarst lakes is currently absent.

Among the various techniques for assessing the size fractionation of solutes among natural colloids, dialysis and ultrafiltration are among the most common ones [14,30,31]. In the past, dialysis allowed for quantifying the colloidal fractions of major and trace metals both in natural waters and in laboratory conditions [32–34]. It was also used to isolate the low-molecular-weight fractions of trace metals [35,36] and to characterize the speciation of metals in various aquatic settings, from lakes to groundwater and sediment pore waters [37–39].

To obtain a better understanding of the OC and major and trace element partitioning among the total dissolved (<0.45 μm), colloidal (1 kDa–0.45 μm), and low-molecular-weight, potentially bioavailable (LMW_{<1kDa}) forms in the thermokarst lakes of Western Siberia, we aimed at quantifying the relationships between the colloidal contents of elements and the lake surface area, permafrost coverage (absent, sporadic, isolated, discontinuous, and continuous), pH, and concentration of the main colloidal carriers—DOC, Fe, and Al. We hypothesized that (i) the colloidal forms of major and trace solutes may be sizably controlled by the degree of lake maturation or growth stage and the permafrost distribution

(connection to the groundwaters and allochthonous or autochthonous nature of DOM), and (ii) the colloidal composition of lake waters will be similar to that of soil porewaters and rivers from the same region provided that the DOC, Fe, Al, and pH levels of these waters are comparable to each other. We anticipate that testing these hypotheses and assessing the colloidal status of solutes across a sizable permafrost and climate gradient will allow for integrating the acquired knowledge into pan-Arctic biogeochemical models of carbon and metal pools, fluxes, and bioavailabilities in surface waters.

2. Materials and Methods

2.1. Study Sites in Western Siberia

The West Siberian Lowland (WSL) includes the taiga, southern forest tundra, and northern tundra biomes, which include two main mire types. The first type is palsa mires on flat frozen peatlands, where thermokarst lakes are highly abundant, covering between 10 and 40 % of the land area. This includes the three most northern regions, i.e., the sporadic, discontinuous, and continuous permafrost zones. The second type of landscape is raised bogs and ridge-pool complexes, which are located in the isolated and sporadic permafrost zones [40]. The main mineral substrates underlying the frozen peat layers of the WSL vary from sands in the south (permafrost-free zone and isolated and sporadic permafrost zones) to silt/loam in the discontinuous permafrost zone, and quaternary clays and loams in the continuous permafrost zone.

Lakes were sampled in the south–north profile of Western Siberia, therefore encompassing different permafrost zones: the southern site in the vicinity of Kogalym town (isolated permafrost zone); the vicinity of Khanymey village (sporadic permafrost zone); the vicinity of Urengoy town (discontinuous permafrost zone); and the most northern key site, in the vicinity of Tazovsky town (tundra biome of the continuous permafrost zone) (Figure 1). Moreover, to compare the colloidal status of the solutes in the lake waters from the permafrost-affected and permafrost-free territories of the WSL, lake waters from the vicinity of Strezhevoy town (the most southern, permafrost-free zone) were collected. The five sampling points belong to the catchments of the four largest northern rivers of Western Siberia—Ob, Pur, Nadym, and Taz. The mean air temperatures (MATs) are -2.5 , -4.0 , -5.6 , -6.4 , and -9.1 °C in the permafrost-free, isolated, sporadic, discontinuous, and continuous permafrost zones, respectively [41]. Further descriptions of the Western Siberia peatlands can be found in former works [14,16,42,43].

Along the south–north profile, we visited 38 lakes during the base flow hydrological period in summer (first half of August). In this regard, the present work represents a snapshot approach to characterizing the colloidal status of lake solutes. The seasonal variations in the thermokarst lake solutes have been extensively studied in previous works of our group [15,16]. However, assessing the seasonal aspects of the colloidal parameters across the entire permafrost gradient was cost-prohibitive and should constitute the subject of further research.

We sampled 10, 10, 8, and 8 lakes in the isolated, sporadic, discontinuous, and continuous permafrost zones, respectively, and 2 lakes in the permafrost-free zone. To reveal the relationship between the colloidal status of the elements and the stage of development (maturation), lakes of different surface areas were selected. The lake maturation or growth stage represents the stage of the thermokarst lake development cycle. This cycle starts from soil subsidence and lichen and moss submergence, followed by peat abrasion and the lateral spreading of shallow water bodies, to the formation of mature lakes, up to several km² in surface area. The terminal stage corresponds to a mature thermokarst lake that can be drained into another lake or into the hydrological riverine network. After that, the new palsa formation via moss colonization and peat formation at the drained lake bottom marks the start of a new cycle.

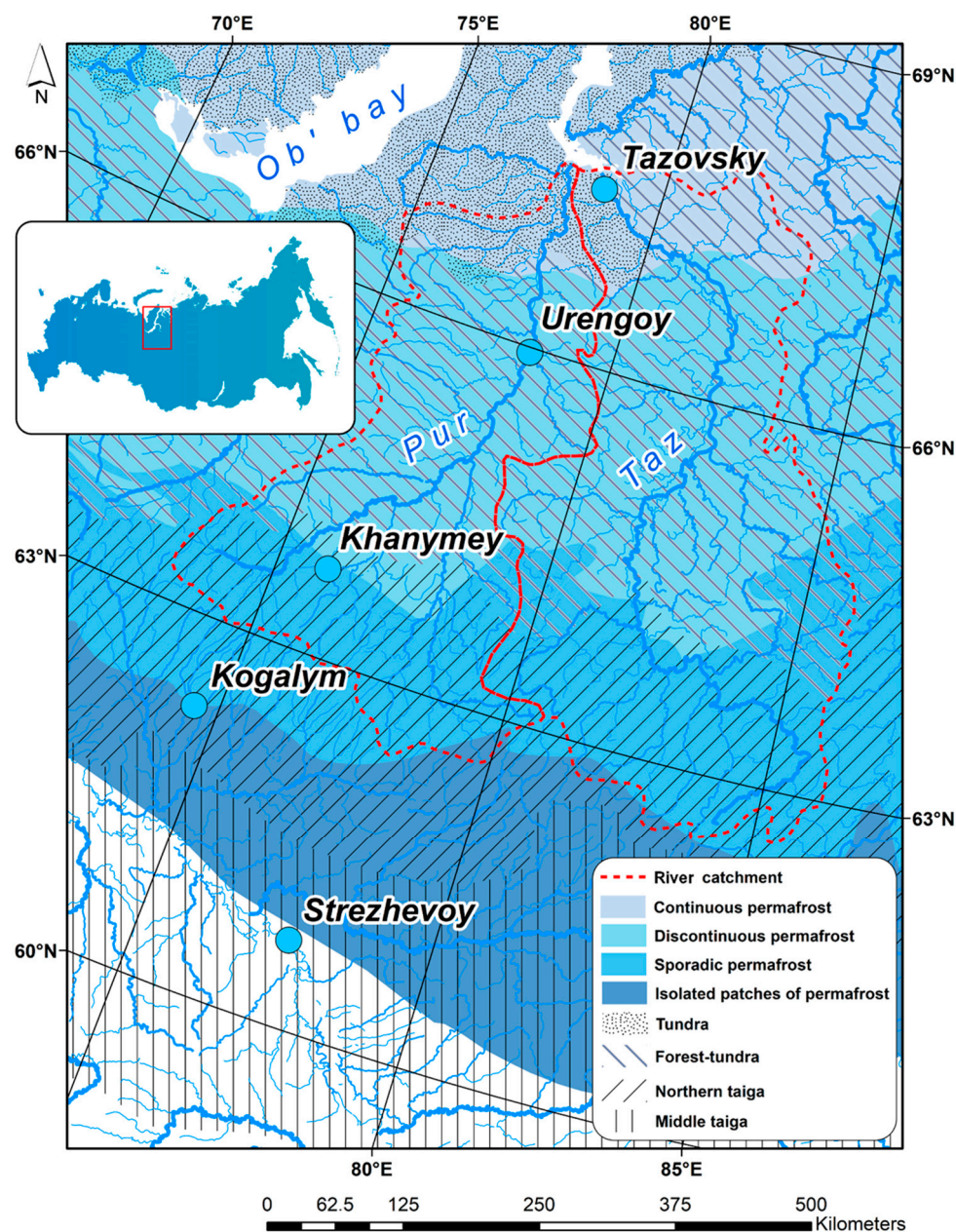


Figure 1. Geographical position of the lake sampling sites in the Western Siberia Lowland (WSL).

The depths of the lakes range from 0.5 to 1.5 m. The lakes are isolated (no inlet or outlet) and ice-covered between 5 and 6 months of the year. Most of them are located within the frozen palsa peatbog. In the Kogalym area, the lakes are within the typical wetland (lake-ridge) complex of the WSL. Note that due to their shallow depth, areal exposure, and strong subjection to wind mixing, all studied lakes lack thermal and chemical stratification and freeze solid in winter. As such, there was no need to consider turnover events when assessing the colloidal status of the lake solutes. Further descriptions of the lake morphology, surface area, depth, and basic hydrochemical parameters are provided elsewhere [16].

2.2. Water Sampling and Size Fractionation

Water samples were taken from a 10 to 20 cm depth via pre-cleaned jars and single-use vinyl gloves. The water samples were taken at the same location as the in situ dialysis experiments using an inflatable boat in order to avoid disturbances of the lake sediments. The water was filtered in situ immediately after sampling through a disposable Sartorius

filter (0.45 μm), and the first 20 to 30 mL of the filtrate was discarded. The filtrates were collected into polypropylene Nalgene vials (15 and 35 mL). These vials were pre-cleaned with HCl and Milli-Q water in a clean room (class A 10,000). For cation analysis by inductively coupled plasma mass spectrometry (ICP MS), the filtrate was acidified with bidistilled HNO_3 . No acidification was used for preserving the filtrates in the second vial, for the dissolved inorganic carbon (DIC), DOC, anion, and ultraviolet (UV) absorbance measurements. The samples were stored in a refrigerator at 4 $^\circ\text{C}$ for 1–2 weeks before analyses. The temperature, pH, and specific electrical conductivity (S.C.) were measured in the field (Multi 3430 m, WTW, Weilheim, Germany). Dialysis experiments were performed in situ, in the lake water, using pre-conditioned 20 to 50 mL dialysis bags (1 kDa or 1.4 nm, regenerated cellulose of Spectra Por 7[®], Shanghai, China). Milli-Q water blanks were routinely run both in the field and in the laboratory to account for possible contamination and to better define the detection limits of the trace element analyses. Dialysis bags were placed in the lake water for 90–100 h in accordance with previous methods [12,13,30,44,45]. Dialysis bags were deployed 1–2 m offshore the coast, in a wave-protected zone, at a depth of 10 to 20 cm from the surface. The wind-induced weak currents led to gentle agitation of the bags, thus facilitating the diffusional exchange of solutes across the membrane.

The percentage of colloids (1 kDa–0.45 μm) of the i -th element was calculated as:

$$([i]_{0.45 \mu\text{m}} - [i]_{1 \text{kDa}}) / [i]_{0.45 \mu\text{m}} \times 100\%, \quad (1)$$

where $[i]_{0.45 \mu\text{m}}$ and $[i]_{1 \text{kDa}}$ are i -th element concentrations in the 0.45 μm filtrate and the 1 kDa dialysate, respectively.

2.3. Analyses

The concentrations of major and trace solutes were measured by methods developed for samples rich in organic matter and low-salinity waters [14]. The concentrations of chemical elements were measured by ICP MS (Agilent Technologies 7500 ce, Santa Clara, CA, USA) with an In+Re internal standard and an error of $\pm 5\%$. During the ICP MS analysis, the SLRS-5 international standard [46] was measured at the beginning and end of the analytical session to assess the external accuracy and verify the sensitivity of the instrument. All certified major (Ca, Mg, K, Na, and Si) and trace element (Al, As, B, Ba, Co, Cr, Cu, Fe, Ga, Li, Mn, Mo, Ni, Pb, all naturally-occurring REEs (La, Ce, Pr, Nd, Sm, Eu, Gd, Dy, Ho, Er, Tm, Yb, Lu), Sb, Sr, Th, Ti, U, V, and Zn) concentrations of the SLRS-5 standard and the measured concentrations agreed, with an uncertainty of 10–20%. The agreement for Cd, Cs, and Hf was between 30 and 50%. For all major and most trace elements, the concentrations in the blanks were below the analytical detection limits (≤ 0.1 – 1 ng L^{-1} for Cd, Ba, Y, Zr, Nb, REE, Hf, Pb, Th, and U; 1 ng L^{-1} for Ga, Ge, Rb, Sr, and Sb; $\leq 10 \text{ ng L}^{-1}$ for Ti, V, Cr, Mn, Fe, Co, Ni, Cu, Zn, and As). Some rare elements, such as Sn, Nb, W, Tl, Ta, and Bi, which were not certified in the reference materials, were also measured, but their concentrations were presented only in the case when 3 independent subsamples provided a $< 20\%$ agreement.

The DOC concentrations were measured by TOC-VCSN (Shimadzu), with an uncertainty of 3% and a detection limit of 0.1–0.05 mg L^{-1} . The DIC was measured by a total organic carbon analyzer (TOC-VCSN, Shimadzu, Kyoto, Japan) (acid addition without combustion), with a detection limit of 0.01 mM and an uncertainty of 5%. Major anion concentrations (Cl and SO_4) were measured by high-performance liquid chromatography (HPLC, Dionex ICS 2000, San Jose, CA, USA), with an uncertainty of 2% and a detection limit of 0.03 mg L^{-1} . Internationally certified water samples (ION-915, MISSISSIPPI-03, RAIN-97, Pérade-20, National Water Research Institute of Canada) were used to check the validity and reproducibility of the DIC analysis. There was good agreement between our replicated measurements and the certified values obtained (relative difference $< 10\%$). The ultraviolet radiation absorption at 254 nm was evaluated using a Bruker CARY-50 UV-VIS spectrophotometer (Agilent Technologies, Santa Clara, CA, USA) and a 10 mm quartz cuvette.

2.4. Statistical Treatment

The data were checked for normality using a Shapiro–Wilk test. The mean and standard deviation values (mean \pm standard deviation) were used to describe the uncertainty of the data. We tested correlations between the element concentrations using the Spearman coefficient (R_s) ($p < 0.05$). This test was also used to check for the impact of external factors (lake water area, latitude) on the percentage of colloids. Further, a pairwise comparative analysis was run via a non-parametric Mann–Whitney test (U-test) to detect the differences among the independent datasets. All plots were built using MS Excel 2016 and the Statistica-12 software package (<http://www.statsoft.com> (accessed on 20 October 2019)).

2.5. Element Speciation Modeling

Element speciation in the presence of major colloidal constituents was assessed using the Visual MINTEQ computer code ([47], version 3.0 for Windows) employing the NICA–Donnan humic ion binding model [48–52]. We assumed that the DOM in the <1 kDa fraction consisted of fulvic acid (FA) and the DOM in the colloidal 1 kDa– 0.45 μm fraction consisted of humic acid (HA). This was based on SUVA₂₅₄ measurements in the <0.45 μm and LMW _{<1 kDa} fractions of the lake water (see Section 3.1 below).

3. Results and Discussion

3.1. Effect of Lake Surface Area on the Colloidal Status of Solutes in Thermokarst Lake Waters

The concentrations of major and trace solutes in the total dissolved (<0.45 μm) and LMW _{<1 kDa} forms in the lake waters of Western Siberia are provided in Table A1. Regardless of the type of permafrost coverage, the SUVA₂₅₄, which is an indicator of the DOC aromaticity and origin, was systematically lower in the <1 kDa dialysates compared to the total dissolved (<0.45 μm) filtrates (Figure S1). This allows us to tentatively consider the colloidal fraction as being dominated by humic material and the LMW _{<1 kDa} fraction as of essentially fulvic nature.

The water surface area is one of the key characteristics of thermokarst lakes and is known to affect the composition of the water, the content of DOM, and the physicochemical parameters [11,13,15,16,43], therefore controlling the colloidal status of the chemical elements [14]. Note that the lake circumference would be also a suitable parameter to trace the degree of coastal peat abrasion given that the peat of the watershed is a main source of solutes in the lakes. However, in addition to the physical abrasion of coastal material, the delivery of colloids via suprapermafrost flow from the lake watershed is also an important source of DOM and related elements [25,42]. This source is better approximated by the lake surface area, given that the exact lake watershed area cannot be quantified in the very flat and permafrost-affected part of the WSL.

Therefore, to characterize the colloidal fractions of trace elements, we carried out a correlation analysis between the lake area (S_{lake}) and the percentage of colloidal elements using the Spearman coefficient ($p < 0.05$); the results are listed in Table S1. In the isolated permafrost zone, with an increase in the lake area, the percentages of the colloidal fractions of Li ($R_s = -0.66$), Mg ($R_s = -0.65$), and Cd ($R_s = -0.71$) decreased. In the sporadic permafrost zone, with an increase in the S_{lake} , the percentage of the colloidal fraction of only DOC increased ($R_s = 0.77$), whereas those of other elements were not affected by the S_{lake} . In the discontinuous permafrost zone, with an increase in the area of lakes, the percentages of the colloidal fractions of Na ($R_s = 0.79$), Cr ($R_s = 0.74$), some REEs ($R_s = 0.82$ – 0.9), and U ($R_s = 0.82$) increased, and the percentages of the colloidal fractions of Mg ($R_s = -0.71$) and Sr ($R_s = -0.79$) decreased. Finally, in the continuous permafrost zone, with an increase in the area of lakes, the percentages of the colloid fractions increased only for Pb ($R_s = 0.74$) and U ($R_s = 0.81$).

The general trends of the colloidal proportions of elements across the entire WSL territory were as follows. Positive and significant ($p < 0.05$) relationships between the lake surface area and the colloidal fractions were found for DOC ($R_s = 0.4$), Ni ($R_s = 0.36$), REEs ($R_s = 0.35$ – 0.48), and Hf ($R_s = 0.48$). Generally, across the Arctic and Subarctic, it

is known that the larger the thermokarst lake, the lower the concentration of DOC and relevant elements because of higher retention times and smaller exchange interfaces with C and metal-rich soils [13,53–55]. In contrast, the contents of the colloidal fractions of Li ($R_s = -0.42$), Mg ($R_s = -0.34$), Ca ($R_s = -0.62$), and Sr ($R_s = -0.41$) decreased with the S_{lake} (Figure 2 and Supplementary Figure S2). In this case, a likely mechanism could be an enhanced release of these soluble alkalis and alkaline-earth elements in the ionic rather than the organic-complexed form. The main source of these elements is shallow groundwater, which is enriched in labile alkalis and alkaline-earth metals either from surrounding clays or carbonate concretions within the sedimentary formations that underlay the peat deposits. The release of underground water is pronounced only at the scale of large lakes and not detectable in small pools and depressions. The latter are fed by shallow peatland porewaters and suprapermfrost waters in which the alkaline earth metals are present as colloidal organic complexes [25].

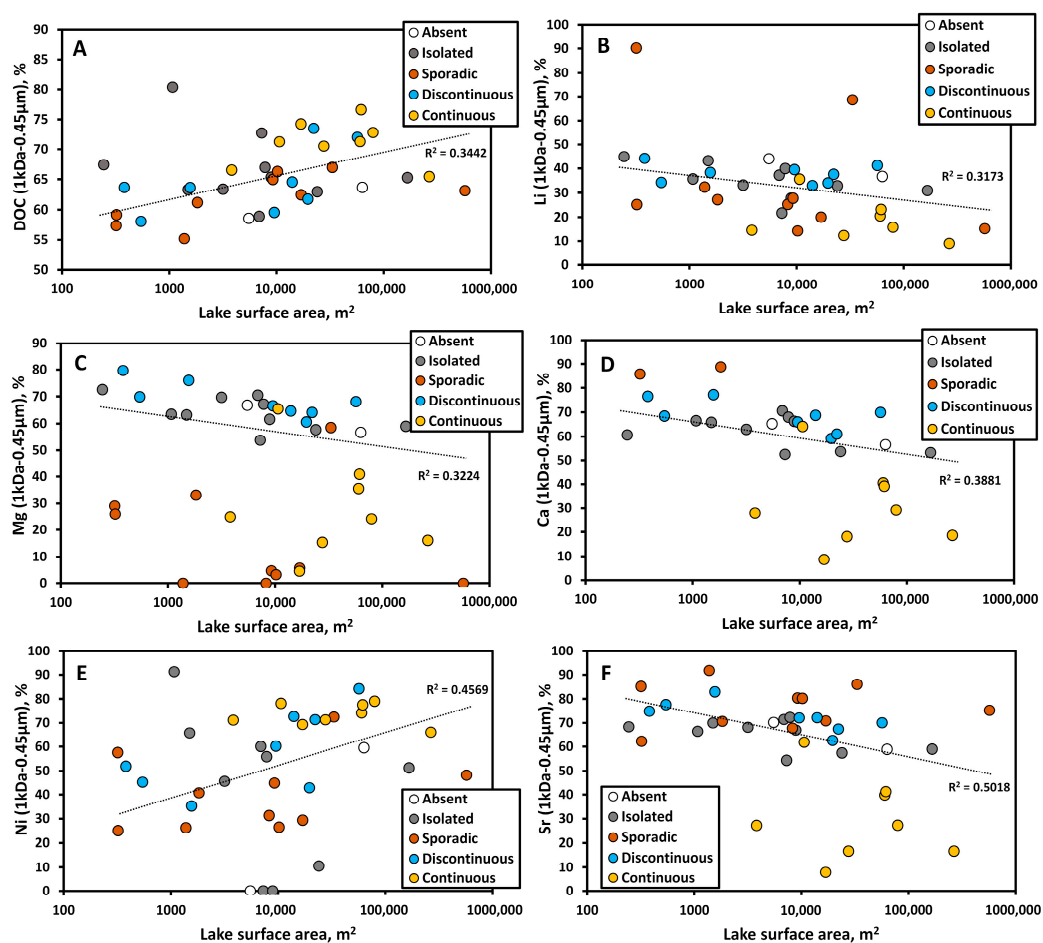


Figure 2. Dependence of colloidal concentrations of DOC (A), Li (B), Mg (C), Ca (D), Ni (E), and Sr (F) in lake waters in all permafrost zones on the lake surface area. The dotted line shows the trendline with the coefficient of determination.

3.2. Groups of Solutes According to Their Colloidal Status and Stoichiometry of Colloids

DOC, Al, and Fe are the main colloid components in the surface waters of Western Siberia [11,12,14]. To distinguish among the three main constituents (DOC, Fe, and Al) that carry trace elements in lake water colloids and to identify the differences among the lakes of the four permafrost zones, we used the Spearman correlations between the pH and the DOC, Al, and Fe concentrations in the total dissolved (<0.45 μm) fraction and the element proportions in the colloidal fraction (Table S2). In the isolated, discontinuous, and continuous permafrost zones, Al exhibited significant correlations with the most trace

elements (Be, Ca, Ti, Cr, Ni, Ga, Sr, Y, Zr, Nb, Ba, REEs, Hf, Pb, Th, and U), while Fe had positive but not significant correlations, and DOC showed no significant correlations with TEs. In the sporadic permafrost zone, DOC exhibited a positive correlation with the colloidal concentrations of Mg, Cr, Ga, As, Sr, Nb, Cd, and Pb, while the strongest relationships with most trace elements were obtained for Al ($R_s > 0.7$ at $p > 0.05$).

The colloidal fraction (1 kDa–0.45 μm) in the lake waters averaged across all permafrost zones of Western Siberia had the following molar stoichiometry: $\text{DOC}_{500 \pm 250} \text{Fe}_{1.6 \pm 1} \text{Al}_{1 \pm 0.8}$. Therefore, given that OC dominated, by more than two orders of magnitude, the mineral constituents of colloids, the role of pure inorganic entities, such as Fe or Al hydroxides, not bound to OM is negligible. Clays were clearly subordinate components of the colloids, given the relatively small (i.e., <10%) fraction of colloidal silica.

The molar OC/Fe/Al stoichiometry of the major colloidal (1 kDa–0.45 μm) carriers changed from 270:1.1:1 in the permafrost-free zone of the WSL to 710:2.3:1 in the isolated, 520:0.8:1 in the sporadic, 430:1.5:1 in the discontinuous, and 640:2.8:1 in the continuous permafrost zone. The average DOC/Fe and Fe/Al molar ratios across latitudes showed maximum values in the sporadic to discontinuous for the former and minimum values for the latter (Figure 3). The highest values of the DOC/Fe ratio in colloids (from 300 to 700) were observed in zones where the peat context was significantly higher, which is confirmed by the previously described DOC concentrations in the lake waters [16], while the minimum ratios were observed in the southern areas free from permafrost. The strong enrichment of Fe in colloids relative to the OC in the permafrost-free zone (Figure 3A) may be due to the formation of Fe(III)-rich high-molecular-weight (HMW) colloids upon the discharge of shallow groundwaters within the lake bottom or at the shores. The Fe(II) present in these groundwaters is quickly oxidized in the surface oxygenated water and forms colloidal Fe(III) oxy(hydroxides) stabilized by DOM [30]. Such a discharge of groundwater is strongly restricted in the permafrost-bearing zone [1,14,56].

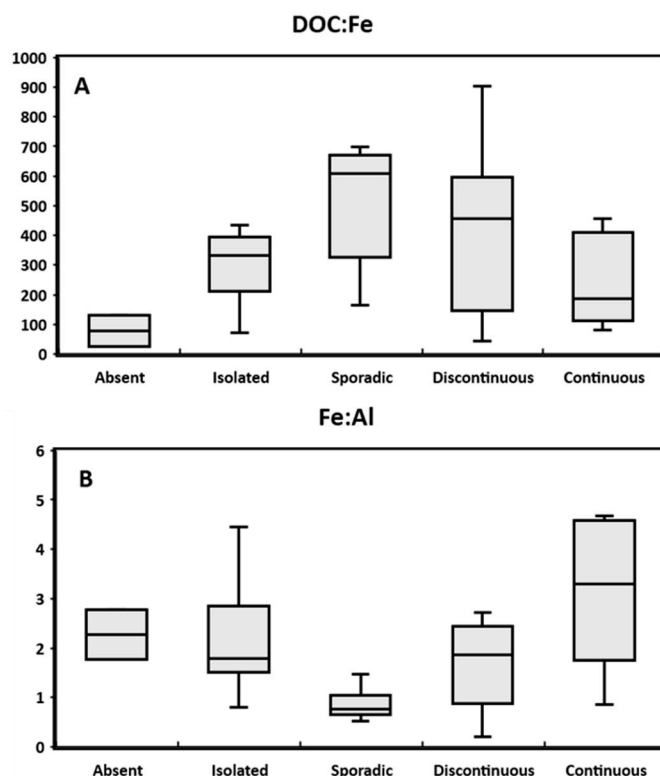


Figure 3. Atomic ratios of DOC/Fe (A) and Fe/Al (B) in colloids (1 kDa–0.45 μm) of Western Siberia lake waters.

Depending on their affinity to colloids and considering both the permafrost-free and permafrost-affected zones, several groups of elements were identified. Members of group 1 were weakly affected by colloids and present mainly (≥ 60 –80%) in the LMW_{<1kDa} fraction. These included alkaline metals (Li, Na, K, and Rb), Ge, Cu, B, As, V, Si, DIC, and Sb. The second group was made up of elements exhibiting a sizable (40–80%) colloidal status: DOC and mobile elements such as alkaline-earth metals (Ca, Mg, Sr, Ba, and Cs), some divalent metals (Ni, Mn, Co, Pb, Zn, and Cd), Cr, Tl, Be, Ga, Hf, U, Mo, and some heavy REEs (Gd, Eu, Tm, and Lu). The third group was trace cations that were present chiefly (≥ 80 %) as colloids: tri- and tetravalent elements hydrolysates (Al, Fe, Y, Ti, Th, and Zr), Nb, and light REEs (Table S3).

It is noteworthy that the lake water pH was found to be an important driver of the colloidal proportions of DOC and alkaline-earth metals (Table S2). We observed a decrease in the metal cations binding to colloids with a lake water pH increase (Figure S3). This is, at first glance, counter-intuitive, given that the colloidal binding of metals generally increases with a rise in pH, as demonstrated by experimental dialysis manipulations with organic-rich natural waters [31]. In the case of the thermokarst lakes of the WSL, however, the highest DOC concentrations were observed in acidic ponds and depressions, at the beginning of lake formation. In these conditions, the majority of metal cations that originated from peat porewaters were present in the form of organic colloids (see Section 3.1). Therefore, we believe that high DOC and low pH in small depressions fed by peat porewater and suprapermafrost flow reflect the terrestrial sources of colloids. In larger lakes, despite higher pH values favorable for metal–OM complexation, the DOC becomes low, the colloidal forms of metals are bio- and photo-degraded, and the overall colloidal binding decreases.

3.3. Element Speciation in Colloids via Thermodynamic Modeling

The results of the vMINTeQ speciation calculations are illustrated in Figure 4. The model predicted a decrease in the DOM complexation degree of some divalent metals (Mg, Ca, Sr, Ba, Ni, Zn, and Mn) in the northern thermokarst lakes compared to the southern (sporadic) permafrost zone, with an increase in pH and a decrease in DOC. Regardless of the size fraction, a fairly high association with the DOM (75–100%) of all metals, except for Rb, Cs, Na, K, Mg, Ca, Sr, and Ba (in the Tazovsky samples; continuous permafrost zone) was observed. However, one has to note that the vMinteq did not account for TEs that were located inside the organo-Fe and organo-Al colloids, i.e., those not adsorbed on the surface of colloidal Fe hydroxides and not complexed to OM. According to other observations, in northern thermokarst thaw ponds, rivers, and soil depressions, a sizeable proportion of trace metals, notably tetravalent (La, Ce, Nd, Yb), and some divalent (Pb, Mn, Co, Ni, Cu, and Cd) cations, are present in the bulk of large-size colloidal Al, Fe-oxy(hydr)oxides stabilized by organic matter [14,24,25].

Therefore, for the quantitative assessment of element associations with organo-ferric colloids, a Fe-normalized empirical TE partition coefficient between the truly dissolved (<1 kDa) and colloidal (1 kDa–0.45 μm) fractions can be defined as:

$$K_d = (\text{TE}/\text{Fe})_{\text{colloidal}} / (\text{TE}/\text{Fe})_{\text{dissolved}} \quad (2)$$

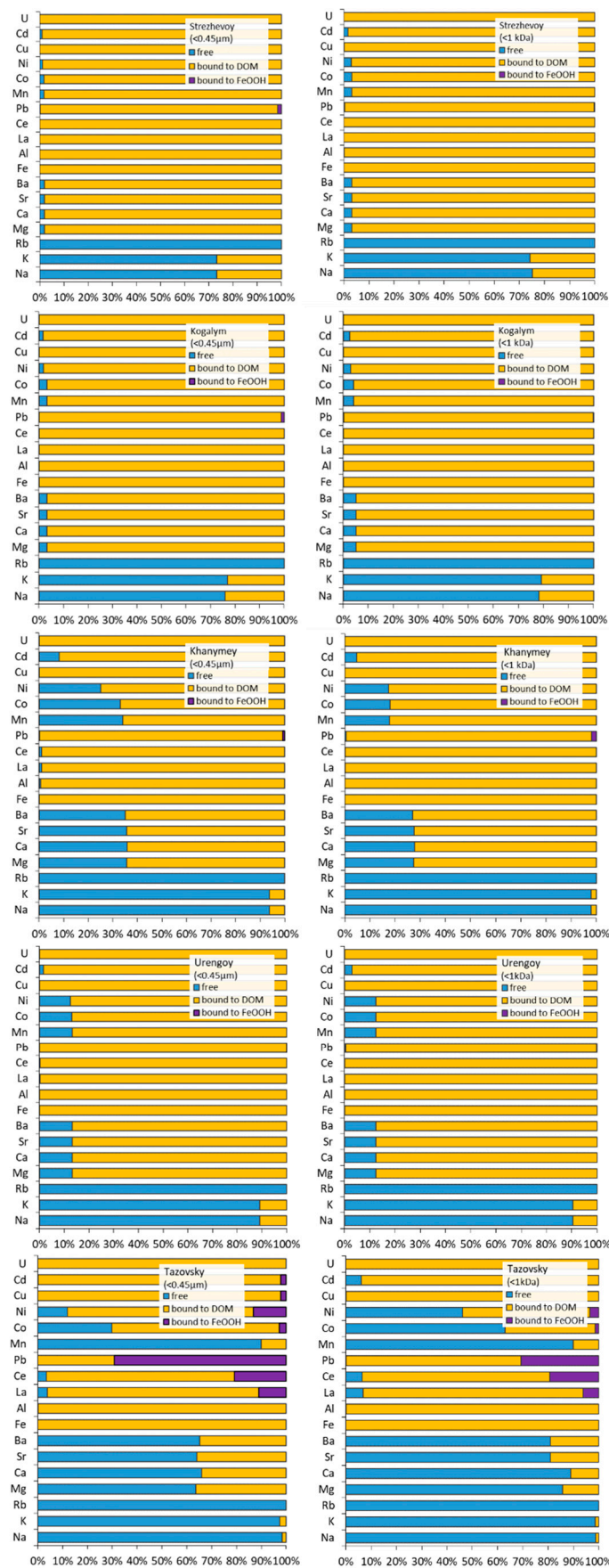


Figure 4. Results of vMinteq calculations of elements speciation in the <0.45 μm fractions (left column) and the <1 kDa fractions (right column). In these calculations, we used the average concentrations of elements in each permafrost zone.

In the WSL lakes, the K_d values of various TEs ranged from 0.6 to 1. Note that there was no statistically significant correlation of the K_d with latitude. For some elements, a correlation of the K_d with the lake surface area was observed. There was a slight increase in the K_d with the S_{lake} for Ti, Co, Ni, and U. With an increase in pH, a slight increase in the K_d was revealed for Ti, Co, and some REEs. It is interesting to note that the TE distribution coefficients calculated from the data of the WSL lakes are comparable to those obtained in laboratory experiments on the co-precipitation of trace elements with solid $\text{Fe}(\text{OH})_3$ in seawater [57,58] and comparable to boreal surface waters of the permafrost-free European Russia, where the average values range from 0.2 to 3.0 [31]. This unambiguously confirms the importance of TE co-precipitation with the dominant component of colloids—Fe(III) oxy(hydr)oxides. This coprecipitation occurs either (1) within the lake sediments, with subsequent diffusion toward the bottom water [44,45], or (2) at the contact zone between surface DOM-rich oxygenated waters and suboxic, Fe(II)-bearing shallow groundwaters seeping at the lake border, as it has been evidenced for rivers and streams of the boreal and subarctic regions [24,59]. Overall, large-sized organo-Fe-Al colloids as the main TE carriers have been evidenced from both macroscopic and spectroscopic observations in the wetlands of various climate zones [60–64].

Note that the low molecular forms of some trace elements, notably of heavy metals exhibiting high concentrations in the snowpack (i.e., Pb, Cd, and Zn), and also Cs and metalloids (Sb and As), may be delivered to the lake water from atmospheric deposition during winter followed by a massive snowmelt in May–June, in a way similar to that in the rivers of the WSL [27].

3.4. Effect of Permafrost Distribution on Colloidal Status of Trace Elements: Possible Evolution in Case of Permafrost Thaw

The dataset acquired in the present study allows us to establish empirical dependence of the element colloidal fractions across the permafrost zones of the WSL (Figure S4, Table S3). There are several spatial patterns of the colloidal fraction contents in the thermokarst lake waters:

(1) Significant ($p < 0.05$) increases in the contents of the colloidal fractions northward were revealed for V ($R_s = 0.35$), Mn ($R_s = 0.54$), Fe ($R_s = 0.47$), Co ($R_s = 0.5$), Ni ($R_s = 0.57$), As ($R_s = 0.44$), Y ($R_s = 0.37$), REEs ($R_s = 0.45\text{--}0.51$), and Hf ($R_s = 0.49$), as illustrated in Figure 5. Note that DOC, Al, Ti, and U also exhibited increases in their colloidal fractions northward, although these increases were not statistically significant;

(2) Significant decreases in the contents of the colloidal fractions from the south to the north were observed for Rb and Li, with a sharp decrease in the percentage of the colloidal fractions from the sporadic to the continuous permafrost zone. Other alkalis and alkaline-earth metals and Si demonstrated similar but not statistically significant latitudinal dynamics;

(3) Elements with a minimum percentage of colloidal fraction in the sporadic permafrost zone: Mg, Ga, Ge, Zr, and Mo;

(4) Other elements that did not show any patterns across the permafrost zones.

A non-parametric Mann–Whitney test (U-test) confirmed sizable differences in the colloidal statuses of solutes among the various permafrost zones (Table S4). The most significant differences were detected between the continuous and other permafrost zones. This likely reflects strong control of environmental factors, such as peat and permafrost thickness, connectivity with the ground waters, the presence of alkaline marine clays, and dominant vegetation.

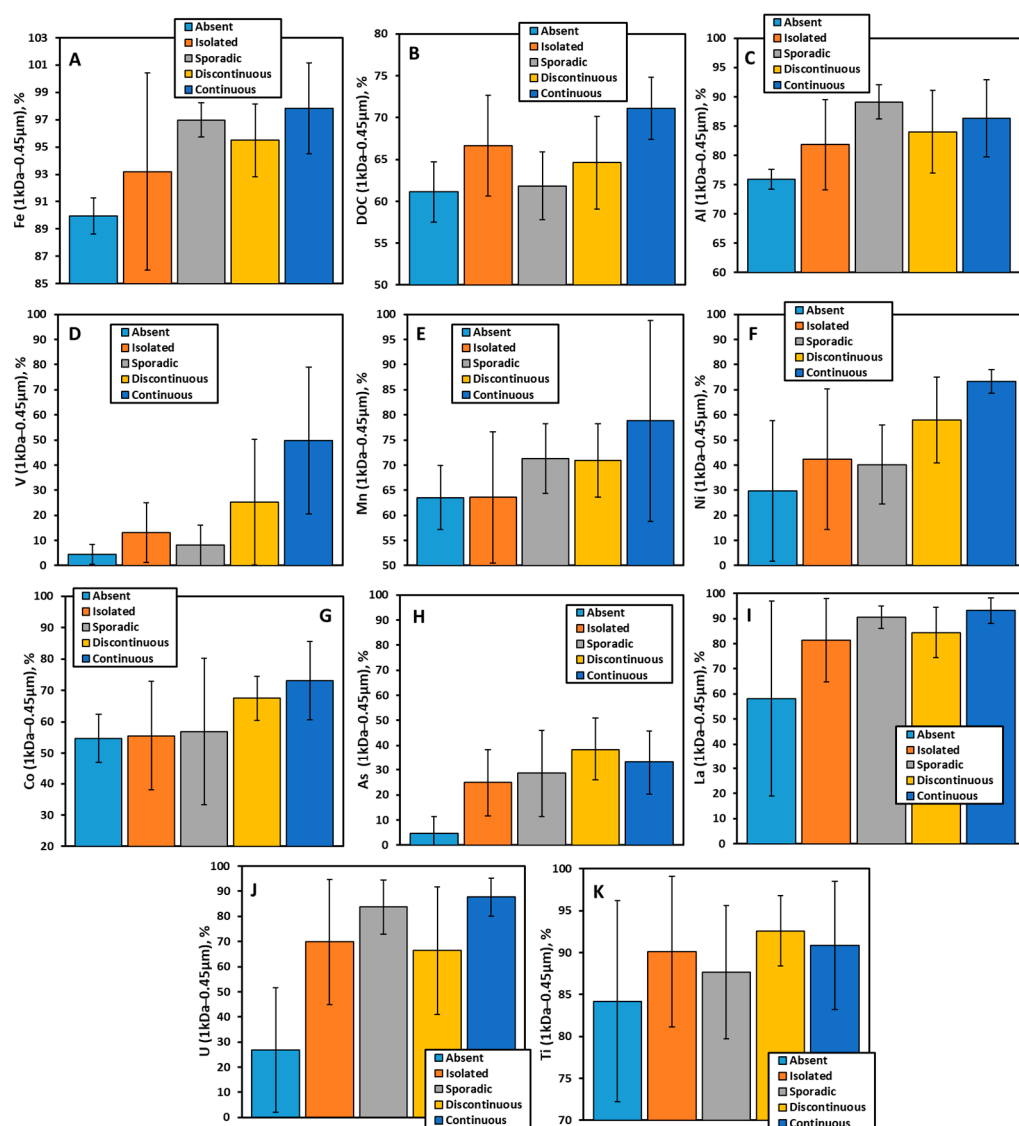


Figure 5. Dependencies of Fe (A), DOC (B), Al (C), V (D), Mn (E), Ni (F), Co (G), As (H), La (I), U (J), and Ti (K) colloidal fraction contents in lake waters across permafrost zones of WSL.

In this work, we observed increases in colloidal-bound trace metals and trivalent and tetravalent hydrolysates from the southern, permafrost-free zones to the northern, permafrost-bearing biomes. Such increases could be linked to a northward increase in the concentration of the main colloidal constituent, the DOC. In the continuous to discontinuous zones, abundant soil (suprapermafrost) waters are located within the peat horizons and travel along the permafrost boundary from the surrounding palsa to the lake [42]. These waters are known to carry sizable amounts of colloidal DOC, Fe, and Al, and also insoluble, low-mobility trace metals [25]. Furthermore, sizable sources of the colloidal material delivered to the thermokarst lakes of the discontinuous and continuous permafrost zones may originate from the thawing of dispersed permafrost ice, which contains large amounts of colloidal material [26]. These organic and Fe- and Al-rich sources of solutes, easily delivered to the lakes over the frozen soil horizons in the northern part of the WSL, are much less abundant in the thawed peat and forest soils of the southern, permafrost-poor part of the region. In contrast, there were decreases in the colloidal fractions of alkali and alkaline-earth metals from the sporadic to continuous permafrost zone. Such decreases could be linked to an abrupt increase in the total dissolved concentration of these elements in the continuous permafrost zone due to the enhanced release of soluble cations from former marine clays overlaid by shallow peat deposits [16].

The colloidal proportions of DOC and inorganic solutes in lake waters revealed in this study can be compared with those measured previously in the river waters [24] and peat porewaters [25] of the WSL cryolithozone (Figure 6). From this comparison, we can conclude generally similar, within ± 10 –20%, contents of the colloidal forms of most solutes (Figure 6). However, a close look at the differences in the colloidal patterns of elements in the various surface waters of the WSL (Table S5) revealed that the lake waters exhibited the highest colloidal contents of DOC, Al, Mn, Si, Zn, and REEs, whereas they were fairly comparable to the rivers and soil waters in terms of the Na, K, Co, Ni, Cu, As, Cd, Th, and U colloidal proportions. These fine differences in the colloidal proportions of various solutes could be explained by the variations in the total ($<0.45 \mu\text{m}$) solute concentrations. For example, the Si concentration is low in lakes due to plankton uptake and high in rivers and soil waters due to contact with clay substrates. As a result, a relatively low capacity of DOC waters to complex minor fractions of Si can be more visible in lakes compared to other waters. Similar explanations can be true for micronutrients such as Mn, Fe, and Zn, whereas higher colloidal contents of Al and REE might reflect a less acidic characteristic of lake waters compared to soil porewaters.

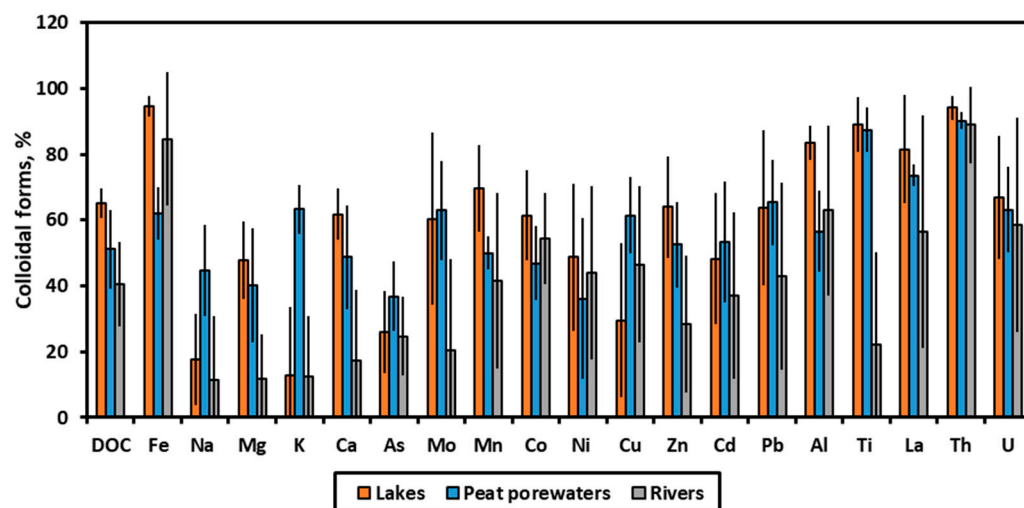


Figure 6. Reported colloidal (1 . . . 3 kDa–0.45 μm) forms of major and trace solutes in peat porewaters [25], rivers [24], and lakes (this study) in the permafrost-affected part of the WSL (mean \pm SD). Other major and trace elements are listed in Table S5 of the Supplementary Materials.

4. Conclusions

A sizable spatial coverage of thermokarst lakes sampled in the Western Siberia Lowland for the total (conventionally) dissolved ($<0.45 \mu\text{m}$) and low-molecular-weight ($<1 \text{ kDa}$) forms using an in situ dialysis procedure allowed for the assessment of the degree of carbon, major, and trace element affinities to organic and organo-mineral colloids depending on the lake size (growth stage), type of permafrost distribution, and basic physico-chemical parameters of the water column (pH and DOC, Fe, and Al concentrations).

Depending on their colloidal status, several groups of elements were identified. Alkaline elements (Li, Na, K, and Rb), Ge, Cu, B, As, V, Si, DIC, and Sb were weakly affected by colloids and present chiefly (≥ 60 –80%) in the $\text{LMW}_{<1\text{kDa}}$ fraction. The second group included elements exhibiting a sizable (40–80%) colloidal status: DOC and mobile elements, including alkaline-earth metals (Mg, Ca, Sr, and Ba), divalent metals (Ni, Mn, Co, Pb, Zn, and Cd), Cr, Tl, Be, Ga, Hf, U, Mo, and heavy REEs. The third group included elements present essentially (≥ 80 %) in the colloidal form, such as tri- and tetravalent element hydrolysates (Al, Fe, Ti, Th, and Zr), Nb, Y, and the majority of REEs.

When averaged across all permafrost zones, the colloidal fractions of organic and inorganic solutes in thermokarst lakes of the WSL were roughly comparable (± 20 %) to those of the peat porewaters and rivers of this region, although for a number of low-mobility

elements (Fe, Al, and REEs), and also Mg, Ca, Mn, Zn, and DOC, the lake waters exhibited systematically higher colloidal fractions compared to the soil waters and rivers. This can stem from both the higher DOC concentrations and low mineralization of lakes, leading to enhanced stability of the colloidal forms of cations.

The climate warming and permafrost thaw in Western Siberia will likely shift the permafrost boundary northwards so that, in the north, the continuous permafrost zone will become discontinuous, while the southern part of the cryolithozone will become permafrost-free. Based on the colloidal status of solutes assessed across the permafrost gradient in the present study, we hypothesize rather moderate (± 10 – 20%) changes in the colloidal proportions of DOC and most major and trace elements. However, colloids in the sporadic permafrost zone may become enriched in DOC relative to Fe, whereas in the continuous permafrost zone, lake colloids may become impoverished in Fe and enriched in Al relative to DOC. The lake water pH, degree of connectivity to groundwater reservoirs, and autochthonous biotic activity may become primary factors controlling the modification of the contents of low-molecular-weight, bioavailable carbon, metal micronutrients, and toxicants in the thermokarst lake waters of Western Siberia.

Supplementary Materials: The following supporting information can be downloaded at: <https://www.mdpi.com/article/10.3390/w15091783/s1>, Figure S1: Box plot (median and IQR range) of SUVA₂₅₄ of the lake water in total dissolved ($<0.45 \mu\text{m}$) and low-molecular-weight (LMW_{<1kDa}) dialysates across the permafrost gradient of the WSL; Figure S2: Dependence of element concentrations in lake waters in all permafrost zones on the water surface area; Table S1: The Spearman correlation coefficients (at $p < 0.05$) of the percentage colloidal forms of elements depending on the lake surface area in different permafrost zones of WSL; Table S2: Correlation matrix (Spearman Rank Order Correlations) of S_{lake} (m^2), pH and DOC, Al, and Fe concentrations ($<0.45 \mu\text{m}$) and percentages of colloidal fractions ($0.45 \mu\text{m}$ – 1kDa) of major and trace elements in lake waters of different permafrost zones of WSL (at $p < 0.05$); Table S3: The groups of elements depending colloidal status in lakes from different permafrost zones of WSL; Figure S3: Some chemical elements whose colloidal status depends on pH level of lake waters; Figure S4: Percentage of the colloidal fraction of chemical elements in lake waters of different permafrost zones of Western Siberia; Table S4: Mann–Whitney U test of the differences in percentages among colloidal fractions in lake water of different permafrost zones. Only statistically significant values are presented (at $p < 0.05$); Table S5: Percentages of measured colloidal (1 – 3kDa – $0.45 \mu\text{m}$) forms in peat porewaters [25], rivers [24], and lakes (this study) in the permafrost affected zones of WSL (mean \pm SD).

Author Contributions: Conceptualization, R.M.M. and O.S.P.; R.M.M., A.G.L. and I.V.K. performed the field sampling; A.G.L. and L.S.S. contributed the data on lakes water chemistry; R.M.M., O.S.P., L.S.S., D.G.K. and T.V.R. analyzed the data; R.M.M. and O.S.P. wrote the original draft and performed reviewing and editing. All authors have read and agreed to the published version of the manuscript.

Funding: This work was supported by the RSF, grant No. 21-77-10067 (90%; lake water sampling, analysis, and interpretation). TR was given partial support from the RFBR, grant No. 19-35-60030. OP was given partial support from the Tomsk State University Development Program “Priority-2030”.

Institutional Review Board Statement: Not applicable.

Informed Consent Statement: Not applicable.

Data Availability Statement: All the data obtained in this work are available in the main text and in the Supplement of this article.

Acknowledgments: The study was carried out using equipment from the Unique Research Installation “System of experimental bases located along the latitudinal gradient” TSU, with financial support from the Ministry of Education and Science of Russia (RF-2296.61321X0043, 13.YHY.21.0005, agreement No. 075-15-2021-672).

Conflicts of Interest: The authors declare no conflict of interest.

Appendix A

Table A1. Physical and chemical parameters and concentrations (mean \pm SD) of elements in lake waters (mg L^{-1} for Cl, SO_4 , DOC, DIC, Na, Mg, K, Al, Si, Ca, Mn, and Fe; $\mu\text{g L}^{-1}$ for all other traces) in total colloidal ($<0.45 \mu\text{m}$) and truly dissolved ($<1 \text{kDa}$) forms in lake waters of different permafrost zones of Western Siberia Lowland (WSL). SC—specific conductivity ($\mu\text{S cm}^{-1}$), SUVA_{254} —specific ultraviolet absorbance ($\text{L mg C}^{-1} \text{m}^{-1}$).

Element	Absent (60°48' N/77°41' E)		Isolated (62°15' N/74°10' E)		Sporadic (63°47' N/75°33' E)		Discontinuous (66°00' N/78°31' E)		Continuous (67°21' N/78°37' E)	
	$<0.45 \mu\text{m}$	$<1 \text{kDa}$	$<0.45 \mu\text{m}$	$<1 \text{kDa}$	$<0.45 \mu\text{m}$	$<1 \text{kDa}$	$<0.45 \mu\text{m}$	$<1 \text{kDa}$	$<0.45 \mu\text{m}$	$<1 \text{kDa}$
SC	16.3 \pm 3.2	–	15.7 \pm 6.6	–	21.6 \pm 8.7	–	22.1 \pm 13	–	20 \pm 9.2	–
pH	4.64 \pm 0.3	–	5.03 \pm 0.7	–	4 \pm 0.2	–	4.11 \pm 0.4	–	6.24 \pm 0.4	–
SUVA_{254}	3.6 \pm 0.8	1.5 \pm 0.6	2.9 \pm 0.5	0.6 \pm 0.3	4.1 \pm 0.5	1.5 \pm 0.6	3.9 \pm 0.4	2.1 \pm 0.3	3.2 \pm 0.6	2.0 \pm 0.1
Cl	0.14 \pm 0.1	0.25 \pm 0.2	0.24	–	–	–	0.19 \pm 0.2	0.29 \pm 0.3	–	–
SO_4	0.49 \pm 0.5	0.36 \pm 0.3	0.21	–	–	–	0.1 \pm 0.06	0.05 \pm 0.01	–	–
DOC	17.4 \pm 3.9	6.7 \pm 0.9	12.1 \pm 3.4	3.97 \pm 1.2	23.6 \pm 10.8	8.6 \pm 4.7	21.3 \pm 5.5	7.56 \pm 2.4	10.1 \pm 1.7	2.94 \pm 0.7
DIC	0.81 \pm 0.2	0.9 \pm 0.03	0.92 \pm 0.6	0.69 \pm 0.2	0.65 \pm 0.1	0.6 \pm 0.1	0.77 \pm 0.2	0.74 \pm 0.2	1.98 \pm 1.1	2.23 \pm 0.98
Li	0.53 \pm 0.3	0.32 \pm 0.2	0.37 \pm 0.4	0.24 \pm 0.26	0.67 \pm 0.4	0.4 \pm 0.1	0.33 \pm 0.2	0.202 \pm 0.1	0.88 \pm 0.5	0.75 \pm 0.4
Be	0.011 \pm 0.01	0.009	0.004 \pm 0.002	0.001 \pm 0.0006	0.02 \pm 0.01	0.04 \pm 0.001	0.006 \pm 0.003	0.002 \pm 0.001	0.008 \pm 0.004	0.001 \pm 0.0007
B	3.94 \pm 1.5	3.54 \pm 1.6	3.17 \pm 1.4	2.27 \pm 1.5	6.27 \pm 2.3	10.4 \pm 3.7	2.22 \pm 1.5	2.36 \pm 1.5	1.68 \pm 1.67	1.97 \pm 2
Na	0.27 \pm 0.2	0.24 \pm 0.1	0.2 \pm 0.1	0.15 \pm 0.09	0.45 \pm 0.4	0.33 \pm 0.1	0.25 \pm 0.3	0.18 \pm 0.16	0.45 \pm 0.2	0.43 \pm 0.2
Mg	0.25 \pm 0.2	0.1 \pm 0.09	0.14 \pm 0.1	0.05 \pm 0.04	0.26 \pm 0.1	0.2 \pm 0.03	0.12 \pm 0.1	0.04 \pm 0.04	1.07 \pm 0.6	0.82 \pm 0.6
Al	0.15 \pm 0.1	0.036 \pm 0.036	0.038 \pm 0.01	0.0065 \pm 0.003	0.092 \pm 0.05	0.0094 \pm 0.004	0.11 \pm 0.08	0.014 \pm 0.007	0.035 \pm 0.03	0.0037 \pm 0.002
Si	0.23 \pm 0.1	0.2 \pm 0.1	0.22 \pm 0.2	0.19 \pm 0.20	0.25 \pm 0.2	0.19 \pm 0.06	0.37 \pm 0.3	0.35 \pm 0.3	0.22 \pm 0.1	0.23 \pm 0.1
K	0.37 \pm 0.5	0.29 \pm 0.3	0.047 \pm 0.04	0.037 \pm 0.027	0.078 \pm 0.071	0.082 \pm 0.02	0.04 \pm 0.02	0.04 \pm 0.02	0.11 \pm 0.1	0.096 \pm 0.1
Ca	0.66 \pm 0.5	0.27 \pm 0.2	0.39 \pm 0.3	0.15 \pm 0.1	0.29 \pm 0.2	0.065 \pm 0.01	0.42 \pm 0.3	0.14 \pm 0.11	2.29 \pm 1.3	1.69 \pm 1.1
Ti	0.51 \pm 0.4	0.056 \pm 0.004	0.3 \pm 0.2	0.025 \pm 0.02	0.8 \pm 0.5	0.07 \pm 0.01	0.8 \pm 0.6	0.044 \pm 0.02	0.49 \pm 0.44	0.02 \pm 0.009
V	0.32 \pm 0.3	0.31 \pm 0.3	0.13 \pm 0.1	0.094 \pm 0.03	1.02 \pm 0.5	0.99 \pm 0.2	0.33 \pm 0.2	0.22 \pm 0.2	0.26 \pm 0.2	0.11 \pm 0.09
Cr	0.38 \pm 0.3	0.19 \pm 0.1	0.15 \pm 0.1	0.23 \pm 0.6	0.52 \pm 0.2	0.29 \pm 0.07	0.31 \pm 0.2	0.12 \pm 0.04	0.19 \pm 0.09	0.039 \pm 0.02
Mn	0.043 \pm 0.04	0.017 \pm 0.02	0.0092 \pm 0.004	0.0032 \pm 0.001	0.013 \pm 0.007	0.0035 \pm 0.002	0.022 \pm 0.02	0.007 \pm 0.006	0.0054 \pm 0.004	0.0008 \pm 0.001
Fe	0.31 \pm 0.3	0.029 \pm 0.03	0.18 \pm 0.2	0.0075 \pm 0.007	0.15 \pm 0.1	0.0039 \pm 0.002	0.35 \pm 0.4	0.0088 \pm 0.005	0.21 \pm 0.1	0.0023 \pm 0.001
Co	0.34 \pm 0.4	0.14 \pm 0.2	0.05 \pm 0.01	0.021 \pm 0.007	0.11 \pm 0.07	0.036 \pm 0.01	0.17 \pm 0.1	0.052 \pm 0.03	0.15 \pm 0.07	0.035 \pm 0.01
Ni	0.66 \pm 0.9	0.29 \pm 0.3	0.096 \pm 0.03	0.065 \pm 0.05	0.35 \pm 0.2	0.19 \pm 0.06	0.45 \pm 0.3	0.15 \pm 0.04	1.21 \pm 0.4	0.32 \pm 0.1
Cu	0.2 \pm 0.2	0.25 \pm 0.1	0.15 \pm 0.07	0.19 \pm 0.09	0.28 \pm 0.1	0.14 \pm 0.04	0.27 \pm 0.2	0.26 \pm 0.04	0.48 \pm 0.3	0.35 \pm 0.07
Zn	6.2 \pm 2.8	2.14 \pm 1.7	2.35 \pm 0.5	1.13 \pm 0.5	4.42 \pm 2.4	1.32 \pm 0.9	5.33 \pm 1.8	1.25 \pm 0.3	1.64 \pm 0.9	0.62 \pm 0.3

Table A1. Cont.

Element	Absent (60°48' N/77°41' E)		Isolated (62°15' N/74°10' E)		Sporadic (63°47' N/75°33' E)		Discontinuous (66°00' N/78°31' E)		Continuous (67°21' N/78°37' E)	
	<0.45 µm	<1 kDa	<0.45 µm	<1 kDa	<0.45 µm	<1 kDa	<0.45 µm	<1 kDa	<0.45 µm	<1 kDa
Ga	0.017 ± 0.008	0.0049 ± 0.004	0.0091 ± 0.004	0.0019 ± 0.001	0.021 ± 0.01	0.0053 ± 0.0009	0.019 ± 0.008	0.0031 ± 0.0009	0.0058 ± 0.005	0.0014 ± 0.001
Ge	0.0019 ± 0.001	0.0014	0.001 ± 0.0007	0.0009 ± 0.0004	0.0035 ± 0.001	0.0033 ± 0.0007	0.001 ± 0.0006	0.0022 ± 0.0009	0.001 ± 0.0008	0.0004 ± 0.0007
As	0.54 ± 0.2	0.56 ± 0.09	0.38 ± 0.1	0.29 ± 0.07	0.47 ± 0.2	0.3 ± 0.09	0.31 ± 0.1	0.18 ± 0.05	0.44 ± 0.1	0.28 ± 0.05
Rb	0.86 ± 1.1	0.59 ± 0.7	0.1 ± 0.096	0.067 ± 0.065	0.15 ± 0.17	0.064 ± 0.05	0.11 ± 0.09	0.077 ± 0.05	0.16 ± 0.1	0.14 ± 0.1
Sr	3.35 ± 3.2	1.32 ± 1.4	2.32 ± 2.4	0.8 ± 0.8	2.72 ± 1.6	0.63 ± 0.4	2.59 ± 2.3	0.78 ± 0.7	9.72 ± 4.9	7.22 ± 4.4
Y	0.053 ± 0.05	0.0083 ± 0.007	0.026 ± 0.03	0.0015 ± 0.001	0.037 ± 0.02	0.0025 ± 0.001	0.06 ± 0.06	0.0026 ± 0.002	0.083 ± 0.03	0.0035 ± 0.002
Zr	0.067 ± 0.07	0.0048 ± 0.004	0.031 ± 0.04	0.0005 ± 0.0003	0.094 ± 0.06	0.0081 ± 0.018	0.088 ± 0.07	0.0041 ± 0.003	0.075 ± 0.04	0.0011 ± 0.0006
Nb	0.0044 ± 0.004	0.0002 ± 0.00004	0.0013 ± 0.0006	0.002 ± 0.004	0.0006 ± 0.0003	0.00004 ± 0.00002	0.0048 ± 0.002	0.0004 ± 0.0003	0.0018 ± 0.0016	0.0001 ± 0.0001
Mo	0.072 ± 0.03	0.015 ± 0.01	0.031 ± 0.04	0.0039 ± 0.002	0.011 ± 0.01	0.0095 ± 0.004	0.045 ± 0.047	0.0084 ± 0.01	0.061 ± 0.052	0.02 ± 0.02
Cd	0.03 ± 0.02	0.013 ± 0.01	0.014 ± 0.006	0.0071 ± 0.004	0.019 ± 0.01	0.015 ± 0.008	0.012 ± 0.003	0.0067 ± 0.004	0.0022 ± 0.002	0.01 ± 0.008
Sb	0.039 ± 0.01	0.055 ± 0.02	0.035 ± 0.008	0.037 ± 0.008	0.043 ± 0.01	0.054 ± 0.01	0.034 ± 0.01	0.042 ± 0.01	0.017 ± 0.007	0.018 ± 0.006
Cs	0.0093 ± 0.005	0.0056 ± 0.003	0.0044 ± 0.004	0.0026 ± 0.002	0.0099 ± 0.007	0.0044 ± 0.003	0.0039 ± 0.004	0.0021 ± 0.002	0.0008 ± 0.0008	0.0005 ± 0.0002
Ba	3.75 ± 4.6	1.48 ± 1.9	1.88 ± 2.1	0.66 ± 0.61	2.84 ± 1.9	0.65 ± 0.4	4.03 ± 3.3	1.16 ± 0.9	1.61 ± 0.64	0.96 ± 0.4
La	0.046 ± 0.06	0.0081 ± 0.006	0.044 ± 0.1	0.0027 ± 0.004	0.02 ± 0.01	0.0015 ± 0.0008	0.047 ± 0.06	0.0024 ± 0.001	0.061 ± 0.03	0.017 ± 0.04
Ce	0.13 ± 0.1	0.02 ± 0.018	0.071 ± 0.15	0.0065 ± 0.01	0.046 ± 0.04	0.0027 ± 0.002	0.12 ± 0.1	0.0053 ± 0.003	0.14 ± 0.07	0.12 ± 0.3
Pr	0.014 ± 0.02	0.0022 ± 0.002	0.0043 ± 0.005	0.0006 ± 0.001	0.0055 ± 0.004	0.0003 ± 0.0002	0.013 ± 0.02	0.0006 ± 0.0004	0.018 ± 0.008	0.0015 ± 0.002
Nd	0.061 ± 0.07	0.0096 ± 0.01	0.018 ± 0.02	0.0027 ± 0.004	0.022 ± 0.02	0.0014 ± 0.0007	0.055 ± 0.06	0.0024 ± 0.002	0.076 ± 0.03	0.0053 ± 0.007
Sm	0.014 ± 0.01	0.0033 ± 0.003	0.0048 ± 0.005	0.0007 ± 0.0008	0.0075 ± 0.005	0.0009 ± 0.0006	0.014 ± 0.01	0.0008 ± 0.0004	0.018 ± 0.009	0.0008 ± 0.0004
Eu	0.0031 ± 0.003	0.0008 ± 0.0006	0.0015 ± 0.0015	0.0002 ± 0.0002	0.0014 ± 0.0009	0.0004 ± 0.0001	0.0035 ± 0.003	0.0005 ± 0.0003	0.0039 ± 0.002	0.0003 ± 0.0003
Gd	0.014 ± 0.01	0.0027 ± 0.002	0.0054 ± 0.006	0.0008 ± 0.0006	0.0068 ± 0.004	0.0008 ± 0.0004	0.013 ± 0.01	0.0011 ± 0.0007	0.018 ± 0.008	0.0036 ± 0.005
Tb	0.002 ± 0.002	0.0003 ± 0.0001	0.0008 ± 0.0008	0.0001 ± 0.0001	0.0011 ± 0.0006	0.0001 ± 0.0001	0.002 ± 0.002	0.0001 ± 0.0001	0.0026 ± 0.001	0.0001 ± 0.0001
Dy	0.011 ± 0.01	0.0017 ± 0.002	0.0049 ± 0.005	0.0006 ± 0.0004	0.0071 ± 0.004	0.0011 ± 0.0006	0.012 ± 0.01	0.0005 ± 0.0003	0.016 ± 0.006	0.0009 ± 0.0002
Ho	0.0019 ± 0.002	0.0003 ± 0.0001	0.0011 ± 0.001	0.0001 ± 0.0001	0.0017 ± 0.001	0.0002 ± 0.0002	0.0024 ± 0.002	0.0001 ± 0.0001	0.003 ± 0.001	0.0001 ± 0.0001
Er	0.005 ± 0.006	0.001 ± 0.0008	0.0032 ± 0.003	0.0003 ± 0.0001	0.0048 ± 0.003	0.0007 ± 0.0002	0.0064 ± 0.006	0.0007 ± 0.0004	0.0083 ± 0.004	0.0004 ± 0.0002
Tm	0.0007 ± 0.0008	0.0002 ± 0.0002	0.0005 ± 0.0005	0.0001 ± 0.0001	0.0008 ± 0.0004	0.0001 ± 0.00004	0.001 ± 0.001	0.0001 ± 0.0001	0.0013 ± 0.0005	0.0001 ± 0.00005

Table A1. Cont.

Element	Absent (60°48' N/77°41' E)		Isolated (62°15' N/74°10' E)		Sporadic (63°47' N/75°33' E)		Discontinuous (66°00' N/78°31' E)		Continuous (67°21' N/78°37' E)	
	<0.45 µm	<1 kDa	<0.45 µm	<1 kDa	<0.45 µm	<1 kDa	<0.45 µm	<1 kDa	<0.45 µm	<1 kDa
Yb	0.0045 ± 0.005	0.001 ± 0.0007	0.0026 ± 0.003	0.0006 ± 0.0007	0.004 ± 0.002	0.0007 ± 0.0005	0.0055 ± 0.0055	0.0004 ± 0.0002	0.0094 ± 0.004	0.0008 ± 0.0003
Lu	0.0006 ± 0.0005	0.0002 ± 0.0001	0.0005 ± 0.0006	0.0001 ± 0.0001	0.0007 ± 0.0004	0.0002 ± 0.0001	0.0007 ± 0.0007	0.0001 ± 0.00004	0.0013 ± 0.0005	0.0001 ± 0.0001
Hf	0.0025 ± 0.003	0.0005 ± 0.0004	0.0016 ± 0.001	0.0005 ± 0.0003	0.0039 ± 0.003	0.0011 ± 0.001	0.0032 ± 0.003	0.0002 ± 0.0001	0.0023 ± 0.002	0.0004 ± 0.0002
Tl	0.0038 ± 0.003	0.002 ± 0.002	0.0019 ± 0.0018	0.0014 ± 0.0009	0.0049 ± 0.003	0.0013 ± 0.0008	0.0016 ± 0.0009	0.0005 ± 0.0004	0.0003 ± 0.0002	0.0002 ± 0.0002
Pb	0.31 ± 0.2	0.22 ± 0.2	0.21 ± 0.1	0.062 ± 0.05	0.19 ± 0.1	0.034 ± 0.02	0.21 ± 0.1	0.063 ± 0.05	0.081 ± 0.09	0.049 ± 0.07
Th	0.011 ± 0.01	0.0005 ± 0.0004	0.0038 ± 0.002	0.0003 ± 0.0002	0.011 ± 0.007	0.0002 ± 0.0002	0.011 ± 0.01	0.0007 ± 0.0005	0.011 ± 0.006	0.0005 ± 0.0003
U	0.0012 ± 0.0007	0.001 ± 0.0008	0.0017 ± 0.001	0.0003 ± 0.0002	0.015 ± 0.03	0.0008 ± 0.0004	0.0019 ± 0.0019	0.0004 ± 0.0002	0.0085 ± 0.006	0.0008 ± 0.0004

References

1. Frey, K.E.; McClelland, J.W.; Holmes, R.M.; Smith, L.C. Impacts of climate warming and permafrost thaw on the riverine transport of nitrogen and phosphorus to the Kara Sea. *J. Geophys. Res. Biogeosci.* **2007**, *112*, G04S58. [\[CrossRef\]](#)
2. Vonk, J.E.; Tank, S.E.; Bowden, W.B.; Laurion, I.; Vincent, W.F.; Alekseychik, P.; Amyot, M.; Billet, M.F.; Canário, J.; Cory, R.M.; et al. Reviews and Syntheses: Effects of Permafrost Thaw on Arctic Aquatic Ecosystems. *Biogeosciences* **2015**, *12*, 7129–7167. [\[CrossRef\]](#)
3. Walvoord, M.A.; Kurylyk, B.L. Hydrologic Impacts of Thawing Permafrost—A Review. *Vadose Zone J.* **2016**, *15*, vzi2016.01.0010. [\[CrossRef\]](#)
4. Wik, M.; Varner, R.K.; Anthony, K.W.; MacIntyre, S.; Bastviken, D. Climate-Sensitive Northern Lakes and Ponds Are Critical Components of Methane Release. *Nat. Geosci.* **2016**, *9*, 99–105. [\[CrossRef\]](#)
5. Turetsky, M.R.; Abbott, B.W.; Jones, M.C.; Anthony, K.W.; Olefeldt, D.; Schuur, E.A.G.; Koven, C.; McGuire, A.D.; Grosse, G.; Kuhry, P.; et al. Permafrost Collapse Is Accelerating Carbon Release. *Nature* **2019**, *569*, 32–34. [\[CrossRef\]](#)
6. Polishchuk, Y.M.; Bogdanov, A.N.; Polishchuk, V.Y.; Manasypov, R.M.; Shirokova, L.S.; Kirpotin, S.N.; Pokrovsky, O.S. Size Distribution, Surface Coverage, Water, Carbon, and Metal Storage of Thermokarst Lakes in the Permafrost Zone of the Western Siberia Lowland. *Water* **2017**, *9*, 228. [\[CrossRef\]](#)
7. Polishchuk, Y.M.; Bogdanov, A.N.; Muratov, I.N.; Polishchuk, V.Y.; Lim, A.; Manasypov, R.M.; Shirokova, L.S.; Pokrovsky, O.S. Minor contribution of small thaw ponds to the pools of carbon and methane in the inland waters of the permafrost-affected part of the Western Siberian Lowland. *Environ. Res. Lett.* **2018**, *13*, 045002. [\[CrossRef\]](#)
8. Serikova, S.; Pokrovsky, O.S.; Laudon, H.; Krickov, I.V.; Lim, A.G.; Manasypov, R.M.; Karlsson, J. High carbon emissions from thermokarst lakes of Western Siberia. *Nat. Commun.* **2019**, *10*, 1552. [\[CrossRef\]](#) [\[PubMed\]](#)
9. Karlsson, J.; Serikova, S.; Vorobyev, S.N.; Rocher-Ros, G.; Denfeld, B.; Pokrovsky, O.S. Carbon emission from Western Siberian inland waters. *Nat. Commun.* **2021**, *12*, 825. [\[CrossRef\]](#) [\[PubMed\]](#)
10. Shirokova, L.S.; Chupakov, A.V.; Ivanova, I.S.; Moreva, O.Y.; Zabelina, S.A.; Shutskiy, N.A.; Loiko, S.V.; Pokrovsky, O.S. Lichen, moss and peat control of C, nutrient and trace metal regime in lakes of permafrost peatlands. *Sci. Total Environ.* **2021**, *782*, 146737. [\[CrossRef\]](#) [\[PubMed\]](#)
11. Pokrovsky, O.S.; Shirokova, L.S.; Kirpotin, S.N.; Audry, S.; Viers, J.; Dupré, B. Effect of permafrost thawing on organic carbon and trace element colloidal speciation in the thermokarst lakes of western Siberia. *Biogeosciences* **2011**, *8*, 565–583. [\[CrossRef\]](#)
12. Pokrovsky, O.S.; Shirokova, L.S.; Kirpotin, S.N.; Kulizhsky, S.P.; Vorobiev, S.N. Impact of western Siberia heat wave 2012 on greenhouse gases and trace metal concentration in thaw lakes of discontinuous permafrost zone. *Biogeosciences* **2013**, *10*, 5349–5365. [\[CrossRef\]](#)
13. Shirokova, L.S.; Pokrovsky, O.S.; Kirpotin, S.N.; Desmukh, C.; Pokrovsky, B.G.; Audry, S.; Viers, J. Biogeochemistry of organic carbon, CO₂, CH₄, and trace elements in thermokarst water bodies in discontinuous permafrost zones of Western Siberia. *Biogeochemistry* **2013**, *113*, 573–593. [\[CrossRef\]](#)
14. Pokrovsky, O.S.; Manasypov, R.M.; Loiko, S.V.; Shirokova, L.S. Organic and organo-mineral colloids in discontinuous permafrost zone. *Geochim. Cosmochim. Acta* **2016**, *188*, 1–20. [\[CrossRef\]](#)
15. Manasypov, R.M.; Vorobyev, S.N.; Loiko, S.V.; Kritzkov, I.V.; Shirokova, L.S.; Shevchenko, V.P.; Kirpotin, S.N.; Kulizhsky, S.P.; Kolesnichenko, L.G.; Zemtsov, V.A.; et al. Seasonal dynamics of organic carbon and metals in thermokarst lakes from the discontinuous permafrost zone of western Siberia. *Biogeosciences* **2015**, *12*, 3009–3028. [\[CrossRef\]](#)
16. Manasypov, R.M.; Lim, A.G.; Krickov, I.V.; Shirokova, L.S.; Vorobyev, S.N.; Kirpotin, S.N.; Pokrovsky, O.S. Spatial and seasonal variations of C, nutrient, and metal concentration in thermokarst lakes of Western Siberia across a permafrost gradient. *Water* **2020**, *12*, 1830. [\[CrossRef\]](#)
17. Pavlova, O.A.; Pokrovsky, O.S.; Manasypov, R.M.; Shirokova, L.S.; Vorobyev, S.N. Seasonal dynamics of phytoplankton in acidic and humic environment in thaw ponds of discontinuous permafrost zone. *Ann. Limnol.—Int. J. Limn.* **2016**, *52*, 47–60. [\[CrossRef\]](#)
18. Pokrovsky, O.S.; Manasypov, R.M.; Pavlova, O.A.; Shirokova, L.S.; Vorobyev, S.N. Carbon, nutrient and metal controls on phytoplankton concentration and biodiversity in thermokarst lakes of latitudinal gradient from isolated to continuous permafrost. *Sci. Total Environ.* **2022**, *806*, 151250. [\[CrossRef\]](#)
19. Audry, S.; Pokrovsky, O.S.; Shirokova, L.S.; Kirpotin, S.N.; Dupré, B. Organic matter mineralization and trace element post-depositional redistribution in Western Siberia thermokarst lake sediments. *Biogeosciences* **2011**, *8*, 3341–3358. [\[CrossRef\]](#)
20. Manasypov, R.M.; Lim, A.G.; Krickov, I.V.; Shirokova, L.S.; Shevchenko, V.P.; Aliev, R.A.; Karlsson, J.; Pokrovsky, O.S. Carbon storage and burial in thermokarst lakes of permafrost peatlands. *Biogeochemistry* **2022**, *159*, 69–86. [\[CrossRef\]](#)
21. Manasypov, R.M.; Shirokova, L.S.; Pokrovsky, O.S. Experimental modeling of thaw lake water evolution in discontinuous permafrost zone: Role of peat, lichen leaching and ground fire. *Sci. Total Environ.* **2017**, *580*, 245–257. [\[CrossRef\]](#) [\[PubMed\]](#)
22. Kuzmina, D.; Lim, A.G.; Loiko, S.V.; Pokrovsky, O.S. Experimental assessment of tundra fire impact on element export and storage in permafrost peatlands. *Sci. Total Environ.* **2022**, *853*, 158701. [\[CrossRef\]](#) [\[PubMed\]](#)
23. Loiko, S.V.; Pokrovsky, O.S.; Raudina, T.V.; Lim, A.; Kolesnichenko, L.G.; Shirokova, L.S.; Vorobyev, S.N.; Kirpotin, S.N. Abrupt permafrost collapse enhances organic carbon, CO₂, nutrient and metal release into surface waters. *Chem. Geol.* **2017**, *471*, 153–165. [\[CrossRef\]](#)

24. Krickov, I.V.; Pokrovsky, O.S.; Manasyrov, R.M.; Lim, A.G.; Shirokova, L.S.; Viers, J. Colloidal Transport of Carbon and Metals by Western Siberian Rivers during Different Seasons across a Permafrost Gradient. *Geochim. Cosmochim. Acta* **2019**, *265*, 221–241. [[CrossRef](#)]
25. Raudina, T.V.; Loiko, S.V.; Kuzmina, D.M.; Shirokova, L.S.; Kulizhskiy, S.P.; Golovatskaya, E.A.; Pokrovsky, O.S. Colloidal Organic Carbon and Trace Elements in Peat Porewaters across a Permafrost Gradient in Western Siberia. *Geoderma* **2021**, *390*, 114971. [[CrossRef](#)]
26. Lim, A.G.; Loiko, S.V.; Kuzmina, D.M.; Krickov, I.V.; Shirokova, L.S.; Kulizhsky, S.P.; Pokrovsky, O.S. Organic Carbon, and Major and Trace Elements Reside in Labile Low-Molecular Form in the Ground Ice of Permafrost Peatlands: A Case Study of Colloids in Peat Ice of Western Siberia. *Environ. Sci. Process. Impacts* **2022**, *24*, 1443–1459. [[CrossRef](#)]
27. Krickov, I.V.; Lim, A.G.; Vorobyev, S.N.; Shevchenko, V.P.; Pokrovsky, O.S. Colloidal associations of major and trace elements in the snow pack across a 2800-km south-north gradient of western Siberia. *Chem. Geol.* **2022**, *610*, 121090. [[CrossRef](#)]
28. Carpita, N.; Sabularse, D.; Montezinos, D.; Delmer, D. Determination of the pore size of cell walls of living plant cells. *Science* **1979**, *205*, 1144–1147. [[CrossRef](#)]
29. Trias, J.; Jarlier, V.; Benz, R. Porins in the cell wall of mycobacteria. *Science* **1992**, *258*, 1479–1481. [[CrossRef](#)]
30. Vasyukova, E.; Pokrovsky, O.S.; Viers, J.; Oliva, P.; Dupré, B.; Martin, F.; Candaudap, F. Trace elements in organic- and iron-rich surficial fluids of the boreal zone: Assessing colloidal forms via dialysis and ultrafiltration. *Geochim. Cosmochim. Acta* **2010**, *74*, 449–468. [[CrossRef](#)]
31. Vasyukova, E.; Pokrovsky, O.S.; Viers, J.; Dupré, B. New operational method of testing colloid complexation with metals in natural waters. *Appl. Geochem.* **2012**, *6*, 1226–1237. [[CrossRef](#)]
32. Magaritz, M.; Wells, M.; Amiel, A.J.; Ronen, D. Application of a multi-layer sampler based on the dialysis cell technique for the study of trace metals in groundwater. *Appl. Geochem.* **1989**, *4*, 617–624. [[CrossRef](#)]
33. Alfaro-De la Torre, M.C.; Beaulieu, P.Y.; Tessier, A.T. In situ measurement of trace metals in lake water using the dialysis and DGT techniques. *Anal. Chim. Acta* **2000**, *418*, 53–68. [[CrossRef](#)]
34. Gimpel, J.; Zhang, H.; Davison, W.; Edwards, A. In situ trace metal speciation in lake surface waters using DGT, dialysis, and filtration. *Environ. Sci. Technol.* **2003**, *37*, 138–146. [[CrossRef](#)]
35. Beneš, P.; Steinnes, E. In situ dialysis for the determination of the state of trace elements in natural waters. *Water Res.* **1974**, *8*, 947–953. [[CrossRef](#)]
36. Jansen, B.; Kotte, M.C.; van Wijk, A.J.; Verstraten, J.M. Comparison of diffusive gradients in thin films and equilibrium dialysis for the determination of Al, Fe(III) and Zn complexed with dissolved organic matter. *Sci. Total Environ.* **2001**, *277*, 45–55. [[CrossRef](#)]
37. Carignan, R.; Rapin, F.; Tessier, A. Sediment porewater sampling for metal analysis: A comparison of techniques. *Geochim. Cosmochim. Acta* **1985**, *49*, 2493–2497. [[CrossRef](#)]
38. Veselý, J.; Majer, V.; Kučera, J.; Havránek, V. Solid–water partitioning of elements in Czech freshwaters. *Appl. Geochem.* **2001**, *16*, 437–450. [[CrossRef](#)]
39. Huerta-Diaz, M.A.; Rivera-Duarte, I.; Sañudo-Wilhelmy, S.A.; Flegal, R. Comparative distributions of size fractionated metals in pore waters sampled by in situ dialysis and whole-core sediment squeezing: Implications for diffusive flux calculations. *Appl. Geochem.* **2007**, *22*, 2509–2525. [[CrossRef](#)]
40. Masing, V.; Botch, M.; Läänelaid, A. Mires of the former Soviet Union. *Wetl. Ecol. Manag.* **2010**, *18*, 397–433. [[CrossRef](#)]
41. Trofimova, I.E.; Balybina, A.S. Classification of climates and climatic regionalization of the West-Siberian plain. *Geogr. Nat. Resour.* **2014**, *35*, 114–122. [[CrossRef](#)]
42. Raudina, T.V.; Loiko, S.V.; Lim, A.; Manasyrov, R.M.; Shirokova, L.S.; Istigechev, G.I.; Kuzmina, D.M.; Kulizhsky, S.P.; Vorobyev, S.N.; Pokrovsky, O.S. Permafrost thaw and climate warming may decrease the CO₂, carbon, and metal concentration in peat soil waters of the Western Siberia Lowland. *Sci. Total Environ.* **2018**, *634*, 1004–1023. [[CrossRef](#)] [[PubMed](#)]
43. Manasyrov, R.M.; Pokrovsky, O.S.; Kirpotin, S.N.; Shirokova, L.S. Thermokarst lake waters across the permafrost zones of western Siberia. *Cryosphere* **2014**, *8*, 1177–1193. [[CrossRef](#)]
44. Pokrovsky, O.S.; Shirokova, L.S.; Zabelina, S.A.; Vorobieva, T.Y.; Moreva, O.Y.; Klimov, S.I.; Chupakov, A.V.; Shorina, N.V.; Kokryatskaya, N.M.; Audry, S.; et al. Size Fractionation of Trace Elements in a Seasonally Stratified Boreal Lake: Control of Organic Matter and Iron Colloids. *Aquat. Geochem.* **2012**, *18*, 115–139. [[CrossRef](#)]
45. Shirokova, L.S.; Pokrovsky, O.S.; Moreva, O.Y.; Chupakov, A.V.; Zabelina, S.A.; Klimov, S.I.; Shorina, N.V.; Vorobieva, T.Y. Decrease of concentration and colloidal fraction of organic carbon and trace elements in response to the anomalously hot summer 2010 in a humic boreal lake. *Sci. Total Environ.* **2013**, *463–464*, 78–90. [[CrossRef](#)]
46. Yeghicheyan, D.; Bossy, C.; Coz, M.B.L.; Douchet, C.; Granier, G.; Heimbürger, A.; Lacan, F.; Lanzanova, A.; Rousseau, T.C.C.; Seidel, J.-L.; et al. A compilation of silicon, rare earth element and twenty-one other trace element concentrations in the natural river water reference material SLRS-5 (NRC-CNRC). *Geostand. Geoanal. Res.* **2013**, *37*, 449–467. [[CrossRef](#)]
47. Gustafsson, J. Visual MINTEQ Ver. 3.1. 2014. Available online: <http://vminteq.lwr.kth.se> (accessed on 8 February 2020).
48. Benedetti, M.F.; Milne, C.; Kinniburgh, D.; van Riemsdijk, W.; Koopal, L. Metal ion binding to humic substances: Application of the non ideal competitive adsorption model. *Environ. Sci. Technol.* **1995**, *29*, 446–457. [[CrossRef](#)]
49. Kinniburgh, D.G.; Van Riemsdijk, W.H.; Koopal, L.K.; Borkovec, M.; Benedetti, M.F.; Avena, M.J. Ion binding to natural organic matter: Competition, heterogeneity, stoichiometry and thermodynamic consistency. *Colloids Surf. A* **1999**, *151*, 147–166. [[CrossRef](#)]

50. Milne, C.J.; Kinniburgh, D.G.; van Riemsdijk, W.H.; Tipping, E. Generic NICA–Donnan Model Parameters for Metal-Ion Binding by Humic Substances. *Environ. Sci. Technol.* **2003**, *37*, 958–971. [[CrossRef](#)]
51. Dzombak, D.A.; Morel, F.M.M. *Surface Complexation Modeling: Hydrous Ferric Oxide*; John Wiley & Sons: New York, NY, USA, 1990.
52. Sjöstedt, C.; Gustafsson, J.-P.; Köhler, S.J. Chemical equilibrium modeling of organic acids, pH, aluminium, and iron in Swedish surface waters. *Environ. Sci. Technol.* **2010**, *44*, 8587–8593. [[CrossRef](#)]
53. Downing, J.A. Emerging global role of small lakes and ponds: Little things mean a lot. *Limnetica* **2010**, *29*, 9–24. [[CrossRef](#)]
54. Holgerson, M.A.; Raymond, P.A. Large Contribution to Inland Water CO₂ and CH₄ Emissions from Very Small Ponds. *Nat. Geosci.* **2016**, *9*, 222–226. [[CrossRef](#)]
55. Arsenault, J.; Talbot, J.; Brown, L.E.; Holden, J.; Martinez-Cruz, K.; Sepulveda-Jauregui, A.; Swindles, G.T.; Wauthy, M.; Lapierre, J.-F. Biogeochemical Distinctiveness of Peatland Ponds, Thermokarst Waterbodies, and Lakes. *Geophys. Res. Lett.* **2022**, *49*, e2021GL097492. [[CrossRef](#)]
56. Pokrovsky, O.S.; Manasypov, R.M.; Loiko, S.; Shirokova, L.S.; Krickov, I.A.; Pokrovsky, B.G.; Kolesnichenko, L.G.; Kopysov, S.G.; Zemtsov, V.A.; Kulizhsky, S.P.; et al. Permafrost coverage, watershed area and season control of dissolved carbon and major elements in western Siberian rivers. *Biogeosciences* **2015**, *12*, 6301–6320. [[CrossRef](#)]
57. Savenko, A.V. Coprecipitation of uranium with iron(III) hydroxide formed in sea water by oxidation of iron (II). *Geochem. Int.* **1996**, *33*, 1–9.
58. Savenko, A.V. Coprecipitation of manganese, copper, zinc, lead and cadmium with iron hydroxide in hydrothermal plumes (by the data of laboratory modeling). *Oceanology* **2001**, *41*, 502–507.
59. Pokrovsky, O.S.; Viers, J.; Shirokova, L.S.; Shevchenko, V.P.; Filipov, A.S.; Dupré, B. Dissolved, suspended, and colloidal fluxes of organic carbon, major and trace elements in the Severnaya Dvina River and its tributary. *Chem. Geol.* **2010**, *273*, 136–149. [[CrossRef](#)]
60. Pourret, O.; Dia, A.; Davranche, M.; Gruau, G.; Héning, O.; Angée, M. Organo-Colloidal Control on Major- and Trace-Element Partitioning in Shallow Groundwaters: Confronting Ultrafiltration and Modelling. *Appl. Geochem.* **2007**, *22*, 1568–1582. [[CrossRef](#)]
61. Pédrot, M.; Dia, A.; Davranche, M.; Bouhnik-Le Coz, M.; Henin, O.; Gruau, G. Insights into Colloid-Mediated Trace Element Release at the Soil/Water Interface. *J. Colloid Interface Sci.* **2008**, *325*, 187–197. [[CrossRef](#)]
62. Guénet, H.; Davranche, M.; Vantelon, D.; Gigault, J.; Prévost, S.; Taché, O.; Jaksch, S.; Pédrot, M.; Dorcet, V.; Boutier, A.; et al. Characterization of Iron–Organic Matter Nano-Aggregate Networks through a Combination of SAXS/SANS and XAS Analyses: Impact on As Binding. *Environ. Sci. Nano* **2017**, *4*, 938–954. [[CrossRef](#)]
63. Ratié, G.; Vantelon, D.; Lotfi Kalahroodi, E.; Bihannic, I.; Pierson-Wickmann, A.C.; Davranche, M. Iron Speciation at the Riverbank Surface in Wetland and Potential Impact on the Mobility of Trace Metals. *Sci. Total Environ.* **2019**, *651*, 443–455. [[CrossRef](#)] [[PubMed](#)]
64. Vantelon, D.; Davranche, M.; Marsac, R.; Fontaine, C.L.; Guénet, H.; Jestin, J.; Campaore, G.; Beauvois, A.; Briois, V. Iron Speciation in Iron–Organic Matter Nanoaggregates: A Kinetic Approach Coupling Quick-EXAFS and MCR-ALS Chemometrics. *Environ. Sci. Nano* **2019**, *6*, 2641–2651. [[CrossRef](#)]

Disclaimer/Publisher’s Note: The statements, opinions and data contained in all publications are solely those of the individual author(s) and contributor(s) and not of MDPI and/or the editor(s). MDPI and/or the editor(s) disclaim responsibility for any injury to people or property resulting from any ideas, methods, instructions or products referred to in the content.